The Eighteenth International Symposium on Artificial Life and Robotics 2013 (AROB 18th '13),
Daejeon Convention Center, Daejeon, Korea, January 30-February 1, 2013

H_∞ controller with graphical LMI region profile for Gantry Crane System

M. Z. Mohd Tumari, M. S. Saealal, M. R. Ghazali and Y. Abdul Wahab[1]

[1]Instrumentation and Control Engineering Research Group (ICE),
Faculty of Electrical and Electronics Engineering, Universiti Malaysia Pahang,
Pekan, Pahang, Malaysia.

[1]zaidimt@ump.edu.my

Abstract: This paper presents investigations into the development of H∞ controller with pole clustering based on LMI techniques to control the payload positioning of INTECO 3D crane system with very minimal swing. The linear model of INTECO 3D crane system is obtained using the system identification process. Using LMI approach, the regional pole placement known as LMI region combined with design objective in H∞ controller guarantee a fast input tracking capability, precise payload positioning and very minimal sway motion. A graphical profile of the transient response of crane system with respect to pole placement is very useful in giving more flexibility to the researcher in choosing a specific LMI region. The results of the response with the controllers are presented in time domains. The performances of control schemes are examined in terms of level of input tracking capability, sway angle reduction and time response specification. Finally, the control techniques is discussed and presented.

Keywords: INTECO 3D crane; sway control; H-infinity; LMI region.

1 INTRODUCTION

The main purpose of controlling an underactuated crane system is transporting the payload in a precise location. However, it is very difficult due to the fact that the payload can exhibit a pendulum-like swinging motion. Various attempts in controlling cranes system based on open loop and closed-loop control system have been proposed. For example, open loop time optimal strategies were applied to the crane by many researchers [1,2]. Poor results were obtained in these studies because open-loop strategy is sensitive to the system parameters and could not compensate for the effect of wind disturbance. In other hand, feedback control which is well known to be less sensitive to disturbances and parameter variations has also been adopted for controlling the crane system. For example, PD controllers has been proposed for both position and anti-swing controls [3]. However, the performance of the controller is not very effective in eliminating the steady state error. In addition, fuzzy logic controller has also been proposed for controlling the crane system by several researchers [4]. However, the fuzzy logic designed still need to struggle in finding the satisfactory rules, membership function, fuzzification and deffuzification parameter heuristically. In addition, since crane system is an underactuated system, sliding mode control also has been proposed by bringing the sliding surface into to the system [5]. Furthermore, the underactuated crane behavior also gives a very challenging problem in achieving good trajectory planning. A few contribution of trajectory planning scheme have been reported in [6]–[12].

In this project, H_∞-synthesis with pole clustering based on LMI techniques is used to control the positioning of payload with very minimal swing. In order to design the controller, the linear model of INTECO 3D crane system as shown in **Fig. 1** is obtained using the system identification process. The reason for choosing H_∞-synthesis is because of its good performance in handling with various types of control objectives such as disturbance cancellation, robust stabilization of uncertain systems, input tracking capability or shaping of the open-loop response. Nevertheless, the weakness of H_∞ controller is in handling with transient response behavior and closed-loop pole location instead of frequency aspects [13]. As we all know, a good time response specifications and closed-loop damping of underactuated crane system can be achieved by forcing the closed-loop poles to the left-half plane. Moreover, many literatures have proved that H_∞ synthesis can be formulated as a convex optimization problem involving linear matrix inequalities (LMI) [14]-[16]. In this case, the normal Riccati equation with inequality condition was used. This behavior will give wide range of flexibility in combining several constraints on the closed loop system. This flexible nature of LMI schemes can be used to handle H_∞ controller with pole placement constraints. In this study, the pole placement constraints will refer directly to regional pole placement [17]. It is slightly difference with point-wise pole placement, where poles are assigned to specific locations in the complex plane based on specific desired time response specifications. In this case, the closed-loop poles of crane system are confined in a suitable region of the complex plane. This region consists of wide variety of useful clustering area such as half-planes, disks, sectors, vertical/horizontal strips, and any intersection thereof [17]. Using LMI approach, the regional pole placement known as LMI region combined with design objective in H_∞ controller should guarantee a fast input tracking capability, precise payload positioning and very minimal sway motion. As an extension of previous work, this report presents a graphical profile of the transient response of crane system with respect to pole placement constraint variation. This graphical analysis is very useful in giving more flexibility to the researcher in choosing a specific LMI region.

The rest of this report is structured in the following manner. The next section provides a description of the linear model of underactuated crane system based on system identification procedure. In section 3, the design of H_∞ controller with pole placement constraint is explained. The graphical profile of crane performance with LMI region variation also discussed in this section. Simulation and experimental validation are reported in Section 4. Finally, concluding remarks are offered in the last section.

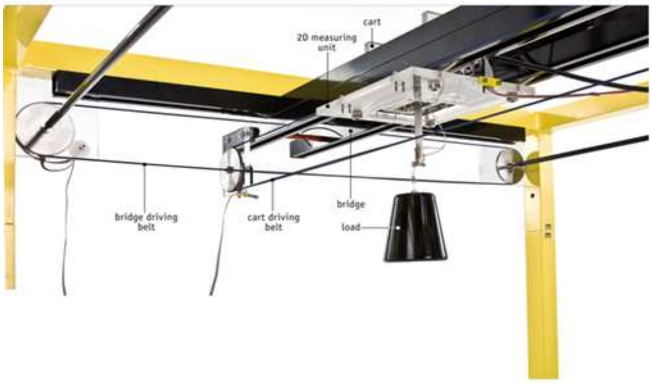

Fig. 1. INTECO 3D Crane.

2 MODELLING OF INTECO 3D CRANE

This section provides a brief description on the modelling of the underactuated crane system, as a basis of a simulation environment for development and assessment of the proposed control scheme. The system identification approach is used to determine the parameter of DC motor for cart position and pendulum behavior for sway motion respectively. In this study, only two-dimensional crane system with payload is considered. In order to have a precise end-point payload motion, the equation of payload position, second order DC motor and pendulum sway motion are described in (1), (2) and (3) respectively

$$x_l = x_c + l\sin\theta \tag{1}$$

$$\ddot{x}_c = -\frac{1}{T}\dot{x}_c + \frac{K}{T}u \tag{2}$$

$$m\ddot{x}_l = -D(\dot{x}_l - \dot{x}_c) - mg\sin\theta \tag{3}$$

where the meaning of different variables is given in **Table 1**.

Table 1: Variable description

Symbols	Meaning
x_l	Payload position
x_c	Cart position
l	Length of the rope
θ	Sway angle
T	Time constant
K	Motor gain
D	Damping constant
m	Mass of the payload
g	Gravity effect
u	Driving voltage

Using the assumption of $\cos\theta \cong 1$ and $\sin\theta \cong \theta$, (1) and (3) can be expressed as follow

$$x_l = x_c + l\theta \tag{4}$$

$$m\ddot{x}_l = -D(\dot{x}_l - \dot{x}_c) - mg\theta \tag{5}$$

Next, by substituting (4) in (5) and (2) respectively, the final equation of motion can be described as

$$\ddot{x}_l = -g\theta - \frac{lD}{m}\dot{\theta} \tag{6}$$

$$\ddot{\theta} = \frac{1}{lT}\dot{x}_l - \frac{g}{l}\theta - \left(\frac{D}{m} + \frac{1}{T}\right)\dot{\theta} - \frac{K}{lT}u \tag{7}$$

Since the design of proposed controller must required the state space representation of the system, equation (6) and (7) are arranged into state space form as shown in (8):

$$\begin{aligned} \dot{x} &= Ax + Bu \\ y &= Cx + Du \end{aligned} \tag{8}$$

Where

$$A=\begin{bmatrix}0 & 1 & 0 & 0\\ 0 & 0 & -g & -\frac{lD}{m}\\ 0 & 0 & 0 & 1\\ 0 & \frac{1}{lT} & -\frac{g}{l} & -\frac{D}{m}-\frac{1}{T}\end{bmatrix} \quad B=\begin{bmatrix}0\\ 0\\ 0\\ -\frac{K}{lT}\end{bmatrix}$$

$C=\begin{bmatrix}1 & 0 & 0 & 0\end{bmatrix}$ $D=[0]$

with state variable $x=\begin{bmatrix}x_l & \dot{x}_l & \theta & \dot{\theta}\end{bmatrix}^T$.

Using simple empirical method in system identification process, the parameters value of crane system are defined as m = 0.732 kg, g = 9.8067 m/s^2, T = 0.0999 s, K = 0.3175 m/s^{2}V, D = 0.0168 and l = 0.4335 m.

3 DESIGN OF H$_\infty$ CONTROLLER WITH LM I REGION

In this study, an integral state feedback control is used as a platform to design the proposed controller. The block diagram of integral state feedback control is shown in **Fig. 2.**

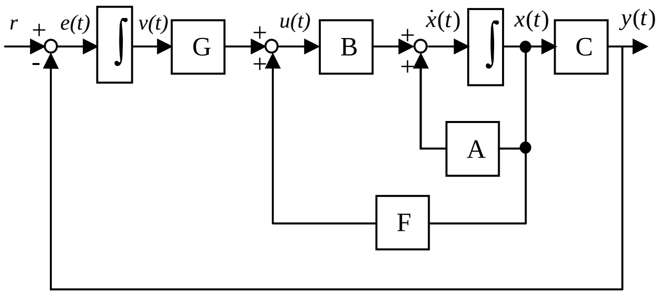

Fig. 2. Block diagram of integral state feedback control.

The main objective of the proposed controller is to find the gain parameter matrix, F and G such that it fulfills the design requirement. From the block diagram of Figure 2, the control input of the system is derived as follow

$$u(t)=Fx(t)+Gv(t) \tag{9}$$

where $v(t)=\int_0^t e(\tau)d\tau$ and $e(t)=r-y(t)$

Using new state variable $x_e=\begin{bmatrix}x^T & v\end{bmatrix}^T$ and equation (9) the representation of state space equation can be rewrite as

$$\begin{bmatrix}\dot{x}(t)\\ \dot{v}(t)\end{bmatrix}=\begin{bmatrix}A & 0\\ -C & 0\end{bmatrix}\begin{bmatrix}x(t)\\ v(t)\end{bmatrix}+\begin{bmatrix}B\\ 0\end{bmatrix}u(t)+\begin{bmatrix}0\\ 1\end{bmatrix}r \tag{10}$$

$$e(t)=r-Cx(t)$$

Next, at the steady state condition as $t\to\infty$, the state space equation can be written in the following form

$$\begin{bmatrix}0\\ 0\end{bmatrix}=\begin{bmatrix}A & 0\\ -C & 0\end{bmatrix}\begin{bmatrix}x(\infty)\\ v(\infty)\end{bmatrix}+\begin{bmatrix}B\\ 0\end{bmatrix}u(\infty)+\begin{bmatrix}0\\ 1\end{bmatrix}r \tag{11}$$

$$0=r-Cx(\infty)$$

By subtracting (10) to (11), the state space form is converted to

$$\begin{aligned}\dot{\tilde{x}}_e(t)&=\tilde{A}\tilde{x}_e(t)+\tilde{B}_2\tilde{u}(t)\\ \tilde{e}(t)&=\tilde{C}_1\tilde{x}_e(t)\end{aligned} \tag{12}$$

where

$$\tilde{A}=\begin{bmatrix}A & 0\\ -C & 0\end{bmatrix},\quad \tilde{B}_2=\begin{bmatrix}B\\ 0\end{bmatrix},\quad \tilde{x}_e=\begin{bmatrix}\tilde{x}\\ \tilde{v}\end{bmatrix}=\begin{bmatrix}x-x(\infty)\\ v-v(\infty)\end{bmatrix}$$

$$\tilde{C}_1=\begin{bmatrix}-C & 0\end{bmatrix},\quad \tilde{e}(t)=e-e(\infty)$$

Then, the new control input function is described as follow

$$\tilde{u}(t)=F\tilde{x}(t)+G\tilde{v}(t)=K\tilde{x}_e(t) \tag{13}$$

Finally, a closed loop state space equation with controller gain, K can be obtained below

$$\begin{aligned}\dot{\tilde{x}}_e(t)&=\tilde{A}_{cl}\tilde{x}_e(t)+\tilde{B}_1 w\\ \tilde{y}(t)&=\tilde{C}_1\tilde{x}_e(t)+\tilde{D}_{11}w+\tilde{D}_{12}u\end{aligned} \tag{14}$$

where

$$\tilde{A}_{cl}=(\tilde{A}+\tilde{B}_2K),\quad \tilde{B}_1=\begin{bmatrix}0 & 0 & 0 & 0 & -1\end{bmatrix},\quad \tilde{D}_{11}=1,$$
$$\tilde{D}_{12}=0$$

and w is exogenous input disturbance or reference input to the system. Let $G_{yw}(s)$ denote the closed loop transfer function from w to y under state feedback control $u=Kx$. Then, for a prescribed closed loop H$_\infty$ performance $\gamma>0$, our constrained H$_\infty$ problem consists of finding a state feedback gain K that fulfil the following objectives:

(1) The closed loop poles are required to lie in some LMI stability region $\mathcal{D}$ contained in the left-half plane

(2) Guarantees the H$_\infty$ performance $\|G_{yw}\|_\infty<\gamma$

Quote from the definition in [13], a subset $\mathcal{D}$ of the complex plane is called an LMI region if there exist a symmetric matrix $\alpha\in\mathbf{R}^{m\times m}$ and a matrix $\beta\in\mathbf{R}^{m\times m}$ such that

$$\mathcal{D}=\{z\in\mathbf{C}:\ f_{\mathcal{D}}(z)<0\} \tag{15}$$

where

$$f_{\mathcal{D}}(z):=\alpha+z\beta+\bar{z}\beta^T$$

Then, pole location in a given LMI region can be characterized in terms of the $m\times m$ block matrix

$$M_{\mathcal{D}}(\tilde{A}_{cl}, X_{\mathcal{D}}) := \alpha \otimes X_{\mathcal{D}} + \beta \otimes (\tilde{A}_{cl} X_{\mathcal{D}}) + \beta^T \otimes \left(\tilde{A}_{cl} X_{\mathcal{D}}\right)^T \quad (16)$$

Quote from the theorem in [10], the matrix $\tilde{A}_{cl}$ is $\mathcal{D}$-stable if and only if there exists a symmetric matrix X such that

$$M_{\mathcal{D}}(\tilde{A}_{cl}, X_{\mathcal{D}}) < 0, \quad X_{\mathcal{D}} > 0 \quad (17)$$

In this study, the region $S(\lambda, r, \theta)$ of complex numbers $x + jy$ such that

$$x < -\lambda < 0, \quad |x + jy| < r, \quad \tan\theta\, x < -|y| \quad (18)$$

as shown in **Fig. 3** is considered.

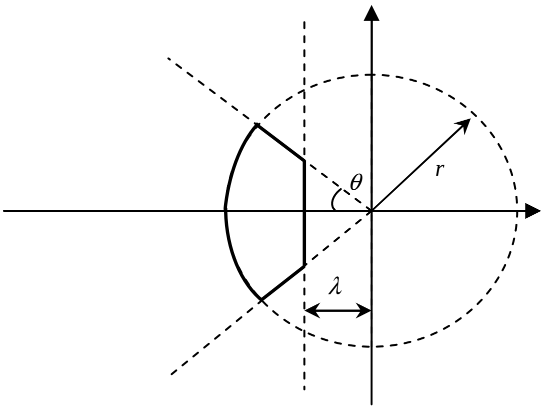

Fig. 3. Region $S(\lambda, r, \theta)$

The advantages of placing the closed loop poles to this region are the cart position response ensures a minimum decay rate λ, a minimum damping ratio $\zeta = \cos\theta$, and a maximum undamped natural frequency $\omega_d = r\sin\theta$ [13]. Equation (19), (20) and (21) show the clustering region used in this study which are λ–stability region, a disk and the conic sector respectively.

$$M_{\mathcal{D}1}(\tilde{A}_{cl}, X_{\mathcal{D}1}) := \tilde{A}_{cl} X_{\mathcal{D}1} + X_{\mathcal{D}1} \tilde{A}_{cl}^T + 2\lambda X_{\mathcal{D}1} < 0 \quad (19)$$

$$M_{\mathcal{D}2}(\tilde{A}_{cl}, X_{\mathcal{D}2}) := \begin{pmatrix} -rX_{\mathcal{D}2} & \tilde{A}_{cl} X_{\mathcal{D}2} \\ X_{\mathcal{D}2} \tilde{A}_{cl}^T & -rX_{\mathcal{D}2} \end{pmatrix} < 0 \quad (20)$$

$$M_{\mathcal{D}3}(\tilde{A}_{cl}, X_{\mathcal{D}3}) :=$$
$$\begin{pmatrix} \sin\theta(\tilde{A}_{cl} X_{\mathcal{D}3} + \tilde{A}_{cl} X_{\mathcal{D}3}^T) & \cos\theta(\tilde{A}_{cl} X_{\mathcal{D}3} - \tilde{A}_{cl} X_{\mathcal{D}3}^T) \\ \cos\theta(X_{\mathcal{D}3} \tilde{A}_{cl}^T - \tilde{A}_{cl} X_{\mathcal{D}3}) & \sin\theta(\tilde{A}_{cl} X_{\mathcal{D}3} + \tilde{A}_{cl} X_{\mathcal{D}3}^T) \end{pmatrix} < 0 \quad (21)$$

where this region is the intersection of three elementary LMI regions ($M_{\mathcal{D}1 \cap \mathcal{D}2 \cap \mathcal{D}3}(\tilde{A}_{cl}, X_{\mathcal{D}})$).

Motivated from the previous work, this study presents an effective way to determine the parameter of region $S(\lambda, r, \theta)$ which in turn bounds the desired maximum overshoot, rise time, settling time, control input and frequency of oscillatory modes. As the transient response profiles varied when the parameter of region is changed, it is suitable to introduce the 3D graphical profiles of LMI region performance. Consider λ is fixed, this investigations only focused on the variation of parameter r and θ. Then, these parameters are chosen based on desired underactuated crane performance from the graphical profile.

Meanwhile, the H_∞ constraint is equivalent to the existence of a solution $X_\infty > 0$ to the LMI

$$\begin{pmatrix} \tilde{A}_{cl} X_\infty + X_\infty \tilde{A}_{cl}^T & X_\infty \tilde{C}_1^T & \tilde{B}_1 \\ \tilde{C}_1 X_\infty & -\gamma I & \tilde{D}_{11} \\ \tilde{B}_1^T & \tilde{D}_{11}^T & -\gamma I \end{pmatrix} < 0 \quad (22)$$

Equation (22) is also known as the Bounded Real Lemma [18]. As mentioned before, the main objective of this study is to minimize the H_∞ norm of $G_{yw}(s)$ over all state feedback gains K that enforce the pole constraints. However, this problem is not jointly convex in the variables $X_{\mathcal{D}1}$, $X_{\mathcal{D}2}$, $X_{\mathcal{D}3}$, X_∞ and K. The convexity can be enforced by seeking a common solution

$$X = X_{\mathcal{D}1} = X_{\mathcal{D}2} = X_{\mathcal{D}3} = X_\infty > 0 \quad (23)$$

to (19)-(22) and rewriting these equations using the auxiliary variable $Y = KX$. These changes of variables lead to the suboptimal LMI approach to H_∞ synthesis with pole assignment in LMI regions. As a result, the new representations of (19)-(22) are shown in the following equation.

$$\mathrm{Herm}[\tilde{A}X + \tilde{B}_2 Y] + 2\lambda X < 0 \quad (24)$$

$$\begin{pmatrix} -rX & \tilde{A}X + \tilde{B}_2 Y \\ * & -rX \end{pmatrix} < 0 \quad (25)$$

$$\begin{pmatrix} \sin\theta(\mathrm{Herm}[\tilde{A}X + \tilde{B}_2 Y]) & \cos\theta(\mathrm{Herm}[\tilde{A}X - \tilde{B}_2 Y]) \\ * & \sin\theta(\mathrm{Herm}[\tilde{A}X + \tilde{B}_2 Y]) \end{pmatrix} < 0 \quad (26)$$

$$\begin{pmatrix} \mathrm{Herm}[\tilde{A}X + \tilde{B}_2 Y] & X\tilde{C}_1^T & \tilde{B}_1 \\ * & -\gamma I & \tilde{D}_{11} \\ * & * & -\gamma I \end{pmatrix} < 0 \quad (27)$$

where $\mathrm{Herm}[\tilde{A}X + \tilde{B}_2 Y] = \tilde{A}X + \tilde{B}_2 Y + X\tilde{A}^T + Y\tilde{B}_2^T$ and $*$ is an ellipsis for terms induced by symmetry [17]. In this study, the entire LMI problem is solved using well known LMI optimization software which is *LMI Control Toolbox*.

Next, to verify the effectiveness of graphical LMI region profile, several specifications have been set up:

- Settling time of 2.5 s with overshoot less than 1% and zero steady state error for the cart movement;

- Sway oscillation is less than ±0.05 rad;
- Control input does not exceed 1 V;

In other words, the designed state feedback gain *K* also must fulfil the mentioned specifications. Computing (24)-(27) using *LMI Control Toolbox*, the graphical profiles of the underactuated crane system performance are depicted in APPENDIX A. In this case, λ is fixed at -3 while the conic sector and disk are varies.

4 SIMULATION AND EXPERIMENTAL VALIDATION

Applying the LMI conditions in (24)-(27) with the advantage of graphical profiles, the parameter of conic sectors and disk that fulfil the design requirement is at $r = 4$ and $\theta = 28^{\circ}$. Then, the state feedback gain, *K* is obtained as followed:

$$K = [-11.2759 \quad -2.9956 \quad 13.6133 \quad 0.9993 \quad 8.42773]$$

with $\gamma = 64.9073$. This state feedback gain also guarantees the H_∞ performance $\|G_{yw}\|_\infty < \gamma$. **Fig. 4** shows that the location of poles has been confined in the selected LMI region. The simulation and experimental validation response of cart position, sway angle and control input are depicted in **Fig. 5**. Close agreement between simulation and experimental results has been successfully achieved. Note that, the cart position response track the desired response of 0.3 m with zero steady state error and settling time of 2.5 s with minimal overshoot. The maximum oscillation of sway angle also has been reduced to ±0.05 rad. Finally, the control input of less than 1 V, has been successfully obtained.

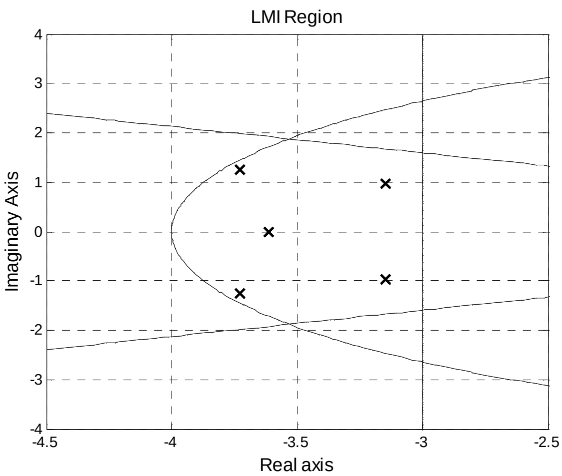

Fig. 4. Location of poles in selected LMI region

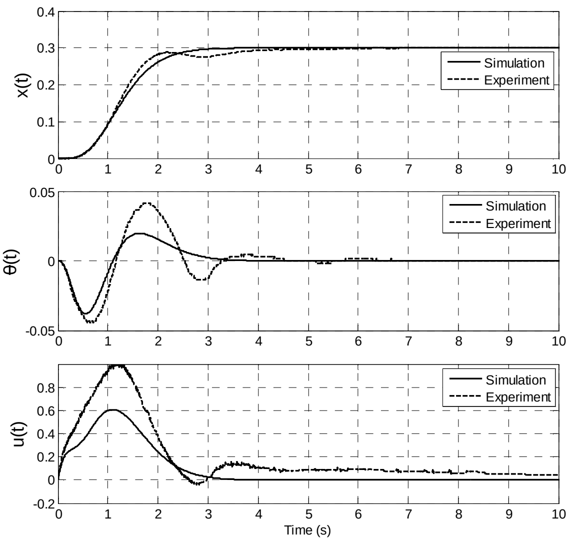

Fig. 5. Response of the underactuated crane system

5 CONCLUSION

This study has introduced new graphical LMI region profile which gives great flexibility in choosing specific parameter of pole placement constraint. The usefulness of this profile has been demonstrated to underactuated crane system using H_∞ synthesis with closed loop pole clustering constraint. This LMI approach has been implemented in the LMI Control Toolbox and validated using INTECO 3D Crane experimental rig with satisfactory results.

REFERENCES

[1] G.A. Manson, "Time-Optimal Control of and Overhead Crane Model," *Optimal Control Applications & Methods*, 3(2), 1992, pp. 115-120.

[2] J. Auernig and H. Troger, "Time Optimal Control of Overhead Cranes with Hoisting of the Load," *Automatica*, 23(4), 1987, pp. 437-447.

[3] H.M. Omar, Control of Gantry and Tower Cranes, M.S. Thesis, Virginia Tech., 2003, Blacksburg, VA.

[4] H.H. Lee and S.K. Cho, "A New fuzzy logic anti-swing control for industrial three-dimensional overhead crane," *Proceedings of the 2001 IEEE International Conference on Robotic and Automation*, 2001, Seoul, pp. 2958-2961.

[5] M. Orbisaglia, G. Orlando, and S. Longhi, "A comparative analysis of sliding mode controllers for overhead cranes," in *Proc. 16th Med. Conf. Control Autom.*, 2008, pp. 670–675.

[6] M.A. Ahmad, A.N.K. Nasir and H. Ishak, "Techniques of anti-sway and input tracking control of a gantry crane system," *IEEE International Conference on Mechatronics and Automation*, pp. 262-267, 2009.

[7] M.A. Ahmad, R.M.T. Raja Ismail, M.S. Ramli, "Hybrid input shaping and non-collocated PID control of a gantry crane system: Comparative Assessment," in *Proc. IEEE/ASME Conf. Adv. Intell. Mechatron.*, 2009, pp. 1792-1797.

[8] M.A. Ahmad, M.S. Ramli, R.M.T. Raja Ismail, A.N.K. Nasir and M.A. Zawawi, "The investigations of PD-type fuzzy logic with different polarities input shaping for anti-sway control of a gantry crane system," in *Proc. of Conference Innovative Technologies in Intelligent Systems and Industrial Applications.*, 2009, pp. 452–457.

[9] M.A. Ahmad, M.S. Saealal, R.M.T. Raja Ismail, M.A. Zawawi, A.N.K. Nasir and M.S. Ramli, "Single input fuzzy controller with command shaping schemes for double-pendulum-type overhead

crane," *AIP conference proceedings*, vol. 1337, no. 1, pp. 113–117, 2011.

[10] M.A. Ahmad, R.M.T. Raja Ismail, M.S. Ramli and N. Hambali, "Comparative assessment of feed-forward schemes with NCTF for sway and trajectory control of a DPTOC," *International Conference on Intelligent and Advanced Systems*, 2010, pp. 1-6.

[11] M.A. Ahmad, R.M.T. Raja Ismail, M.S. Ramli and N. Hambali, "Investigations of NCTF with input shaping for sway control of a double-pendulum-type overhead crane," *Proc. of 2nd IEEE International Conference on Advanced Computer Control*, 2010, pp. 456-461.

[12] M.A. Ahmad, R.M.T. Raja Ismail, M.S. Ramli and N. Hambali, "Analysis of IIR filter with NCTF-PI control for sway and trajectory motion of a DPTOC System," *International Conference on Electronics Devices, Systems and Applications*, 2010, pp. 54-58.

[13] M. Chilali, P. Gahinet, "H_∞ design with pole placement constraints: an LMI approach", *IEEE Transactions on Automatic Control*, Vol. 41(3), pp. 358-367, 1996.

[14] P. Gahinet and P. Apkarian, "A linear matrix inequality approach to H_∞ control," *Int. J. Robust Nonlinear Contr.*, vol. 4, pp. 421-448, 1994; also in *Proc. CDC*, 1993, pp. 656-661.

[15] T. Iwasaki and R. Skelton, "All controllers for the general H_∞ control problem: LMI existence conditions and state-space formulas," *Automatica*, vol. 30, pp. 1307-1317, 1994.

[16] A. Packard, "Gain scheduling via linear fractional transformations," *Syst.Contr. Lett.*, vol. 22, pp. 79-92, 1994.

[17] M. Chilali, P. Gahinet, P. Apkarian, "Robust pole placement in LMI regions", *IEEE Transactions on Automatic Control*, Vol. 44(12), pp. 2257-2270, 1999.

[18] S. Boyd, L. EL Ghaoui, E. Feron and V. Balakrishnan, "Linear Matrix Inequalities in System Control Theory, Vol. 15 of *Studies in Applied Mathematics*, SIAM, Philadelphia, PA, June 1994.

APPENDIX A

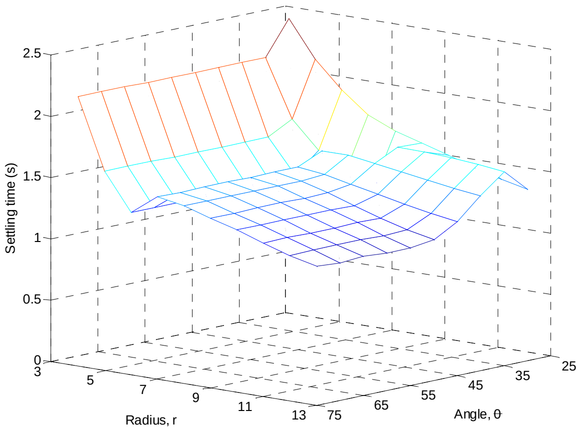

Fig. 6 Settling time profile

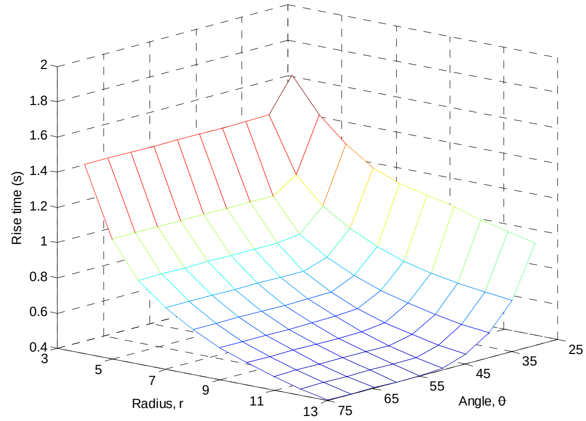

Fig. 7 Rise time profile

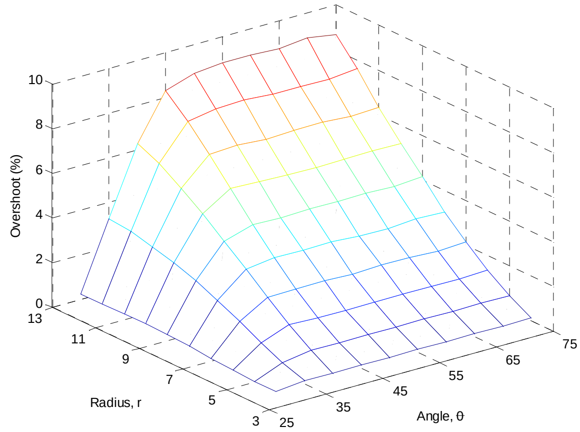

Fig. 8 Overshoot profile

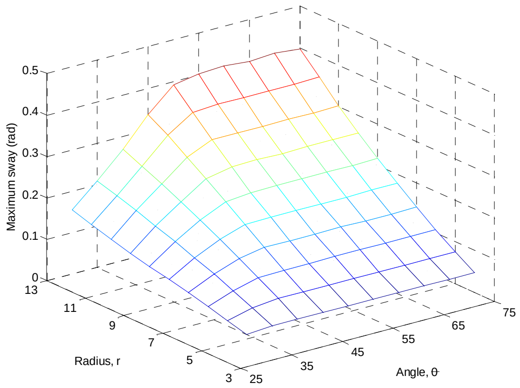

Fig. 9 Maximum sway profile